JOURNAL OF MATERIALS SCIENCE 33 (1998) 1105–1116

Strength and toughness properties of two nitrogen alloyed stainless steels and their submerged arc weldments at cryogenic temperatures

P. DEIMEL, H. FISCHER, M. HOFFMANN
Staatliche Materialprüfungsanstalt, Universität Stuttgart, 70569 Stuttgart, Germany

Submerged arc weldments of the two nitrogen-alloyed stainless steels X2 CrNiN 18 10 (similar to AISI 304 LN) and X4 CrNiMoN 18 14 (similar to AISI 316 LN) welded with the fully austenitic filler metal X2 CrNiMnMoN 20 16 were investigated. Tensile, impact toughness and single-specimen *J*-integral tests at room temperature, 77 K and 4 K were performed. The strength of the materials increased whereas the impact toughness and the fracture toughness decreased with decreasing temperature. The toughness of the steel X4 CrNiMoN 18 14 was superior to that of X2 CrNiN 18 10, and for the austenitic weld a good combination of strength and toughness was also found. On the fracture surface of the compact tension specimens, a stretch zone was found, the width of which was reduced with decreasing test temperature. For all three materials at all three temperatures the critical values, J_{Ic}, of the *J* integral determined according to ASTM E 813 are approximately twice the respective values for the *J* integral at physical crack initiation determined according to the German specification DVM 002 using the width of the stretch zone.

1. Introduction

For the safe design and operation of large cryogenic tanks, e.g., for liquid hydrogen, good strength and toughness properties of the materials used are needed for temperatures down to 20 K (liquid hydrogen temperature). As regards the overall behaviour of such a tank, special attention must be given to the behaviour of the weldments. Owing to the strength, ductility and toughness, even at the lowest temperatures, austenitic stainless steels are used for the construction of large stationary storage vessels for liquid hydrogen [1, 2]. The tensile strength is marked by a strong increase with decreasing temperature. The yield strength is significantly influenced by the nitrogen content. Steels without nitrogen show only a slight increase in the yield strength with decreasing temperature whereas for the nitrogen-alloyed stainless steels a strong increase is found [3]. Nitrogen also increases the stability of the austenitic steel with respect to martensitic transformation [4].

The fracture toughness values at 4 K of austenitic Cr–Ni steels of different strengths fall into a scatter band that is inversely proportional to the yield strength [5,6]. Weldments of the austenitic steels exhibit a strength that is similar or superior to the base metals but the scatter band of fracture toughness for weldments of different strengths is well below the scatter band for the base materials [7]. In particular, with applications where high strength and toughness are needed, new weld metals have been developed and it seems possible that a similar combination of strength and toughness as those of the base materials can be achieved [8].

Microstructural investigations of the toughness behaviour of austenitic weldments have revealed that the fracture toughness at cryogenic temperatures is reduced by δ-ferrite, non-metallic inclusions and precipitation of chromium carbides, causing sensitization [9–11]. An increase in the width of the columnar grains also reduces the fracture toughness [11]. For the economical construction of large storage and transport vessels, welding procedures with a good deposit efficiency (such as the submerged arc (SA) process) are of special interest. Comparing weldments produced by gas tungsten arc (GTA), gas metal arc (GMA) and SA which had δ-ferrite contents of 0.6%, 2.0% and 1.8%, respectively, has revealed low strength and low toughness of the SA weldment [10]. The best toughness and tensile properties were obtained from the GTA weld, followed by GMA welds. The SA welds had the poorest properties. This variation in properties was attributed to the cleanliness of the weld metal depending on the welding process. The SA welds had a higher concentration of non-metallic inclusion than did GTA welds.

The fracture toughness values of austenitic steels published up to now were determined on the basis of the critical value J_{Ic}, of the *J* integral according to ASTM E 813-81 [12] and ASTM E 813-89 [13]. The German specification DVM 002 [14] additionally offers the possibility to determine the *J* integral, J_i, at physical crack initiation. For the determination of J_i, the width of the stretch zone has to be measured by

means of scanning electron microscopy (SEM). Since J_i values were not available in the literature, it was the aim of this investigation to determine the dependence of J_i values on the temperature, down to 4 K, and to compare these values with corresponding J_{Ic} values. Thereby the temperature dependence of the stretch zone width was also investigated.

2. Experimental procedure

2.1. Materials

From plates of the two nitrogen-alloyed stainless steels X 2 CrNiN 18 10 (similar to AISI 304 LN) and X 4 CrNiMoN 18 14 (similar to AISI 316 LN) of 25 mm thickness, SA weldments were prepared by Thyssen Nordseewerke, Emden, Germany, using the fully austenitic filler metal X 2 CrNiMnMoN 20 16. The chemical composition of the stainless steels and of the filler metal are given in Table I, and details of the welding procedures in Table II. The plates had been hot rolled and solution annealed (1050 °C for 25 min and then water quenched). Figs 1 and 2 illustrate the weld build-up of the two seams. The steel X 2 CrNiN 18 10 had a Vickers hardness of 168 HV 10 and a grain size of 125 μm. The heat-affected zone mainly consisted of fine grains (50 μm) with a hardness of 202 HV 10. Some coarse grain (125 μm) regions were found with 172 HV 10 locally to the root and top pass. The steel X 4 CrNiMoN 18 14 had a hardness of 174 HV 10 and a grain size of 65 μm. The heat-affected zone, which contained no coarse grains, had the same grain size and a hardness of 221 HV 10.

2.2. Experimental methods

The tensile behaviour and the toughness properties of the two base materials and the weld metal were evaluated at 295 K (room temperature), 77 K and 4 K. The type and orientation of the specimens used are given in Fig. 3.

For the tensile and fracture mechanics tests at room temperature and 77 K, a conventional 200 kN servohydraulic testing machine was used (with a liquid-nitrogen bath for the tests at 77 K). Testing at 4 K was conducted in a specially designed low-temperature materials-testing system (Fig. 4). Details of this testing facility, consisting of a personal-computer-controlled 200 kN servohydraulic testing machine and a super–insulated double-walled cryostat, have been described in [15].

All tensile tests of the base materials and the weld metal were conducted on cylindrical specimens of 8 mm diameter and a gauge length of 40 mm. The tests at room temperature and 77 K were in accordance with DIN EN 1002-1 [16], whereas the tests at 4 K were performed at a lower strain rate, $\dot{\varepsilon} = 5 \times 10^{-4}\,s^{-1}$, to ensure that the heat developed by the plastic deformation could be removed without

TABLE II Characteristic data of weldments

Weldment 1	
Base material	X 2 CrNiN 18 10 (similar to AISI 304 LN)
Filler metal	UP-X 2 CrNiMnMoN 20 16
Submerged arc welding flux powder	Record NICRO W
Plate thickness	25 mm
Weld seam length	1600 mm
Shape of seam	Double-V seam $\frac{2}{3}$:$\frac{1}{3}$
Weldment 2	
Base material	X 4 CrNiMoN 18 14 (similar to AISI 316 LN)
Filler metal	UP-X2 CrNiMnMoN 20 16
Submerged arc welding flux powder	Record NICRO W
Plate thickness	25 mm
Weld seam length	2070 mm
Shape of seam	Double-V seam $\frac{2}{3}$:$\frac{1}{3}$

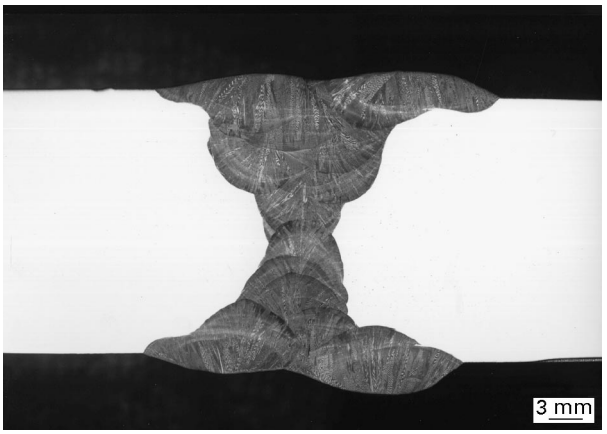

Figure 1 Macrogaph of submerged arc welding of plates from steel X2 CrNiN 18 10, with filler metal X2 CrNiMnMoN 20 16.

TABLE I Composition of base materials and filler metal

Material	Chemical composition (wt%) according to manufacturer								
	C	Si	Mn	P	S	Cr	Mo	Ni	N
Base material X 2 CrNiN 18 10 (similar to AISI 304 LN)	0.022	0.40	1.54	0.024	0.003	17.34	—	9.06	0.16
Base material X 4 CrNiMoN 18 14 (similar to AISI 316 LN)	0.025	0.40	1.46	0.028	0.003	17.07	2.64	13.01	0.16
Filler metal X 2 CrNiMnMoN 20 16	0.013	0.55	7.82	0.014	0.003	20.12	2.86	15.56	0.16

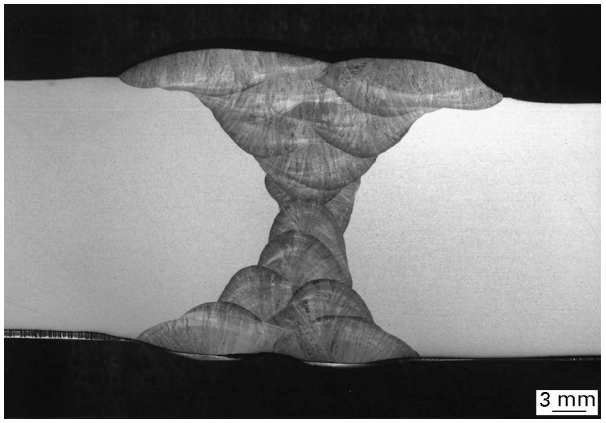

Figure 2 Macrograph of submerged arc welding of plates from steel X4 CrNiMoN 18 14, with filler metal X2 CrNiMnMoN 20 16.

significant temperature increase of the specimen. The strain rate used was within the limits of ASTM E 1450-92 [17]. For comparison, tensile tests at room temperature were also performed at this low strain rate, $\dot{\varepsilon} = 5 \times 10^{-4}\,s^{-1}$.

The impact tests were performed in accordance with DIN EN 10045 [18] using Charpy V-notch (CVN) specimens at room temperature, 77 K and 4 K. For the testing at 4 K (performed by Linde, Höllriegelskreuth, Germany), a special insulation box was used consisting of two shaped parts from polystyrene foam covered with several layers of a superinsulating foil. After the specimen in the box had been cooled with liquid helium, it was also tested in the same box. The impact energy which was absorbed by the box was taken into account by a calibration curve.

J-integral tests on compact tension specimens at room temperature, 77 K and 4 K were carried out using the single-specimen compliance method in accordance with ASTM E 813-81 [12], ASTM E 813-89 [13] and DVM 002 [14]. The specimens of 25 mm thickness were 20% side grooved (in some cases 25%) and pre-cracked at room temperature to an a/W ratio of approximately 0.6, where a and W are the crack length and the width of the specimen, respectively. As in the case of the tensile tests, testing at 4 K was performed with a reduced deformation rate, i.e., the crack-opening displacement rate ($\dot{COD}$) was in the range 0.002–0.004 mm s^{-1} to avoid heating of the specimens. After testing, the end of stable crack advance was marked by fatigue cycling.

The evaluation in accordance with [12, 13] resulted in J_{Ic} values which could be compared with values given in the newer and older literature. From the evaluation according to [14] (using the width of the stretch zone which has to be measured by SEM) the value J_i of the J integral for physical crack initiation was determined.

The fracture appearance of the specimens tested in tensile, impact toughness and fracture mechanics testing was investigated by SEM on a macroscopic and microscopic scale.

3. Experimental results and discussion

3.1. Tensile tests

The stress–strain curves at room temperature and 4 K of the base materials X 2 CrNiN 18 10 and X 4 CrNiMoN 18 14 as well as the weld metal X 2 CrNiMnMoN 20 16 are given in Figs 5–7 and show that the strength increases with decreasing temperature. At 4 K, frequent serrations are observed and the shape of the stress–strain curve for X 2 CrNiN 18 10 is typical for materials that show martensitic transformation during plastic deformation [19]. The strength values together with the elongation at fracture and the reduction in area with respect to temperature are given in Table III and graphically in Figs 8–10. At room temperature, both base materials have similar strengths and ductilities. With decreasing temperature the yield and tensile strength of the steel X 2 CrNiN 18 10 increases more than in the case of the steel X 4 CrNiMoN 18 14. The elongation at fracture and the reduction of area of the steel X 2 CrNiN 18 10 decrease with decreasing temperature. In the case of the steel X 4 CrNiMoN 18 14, the elongation at

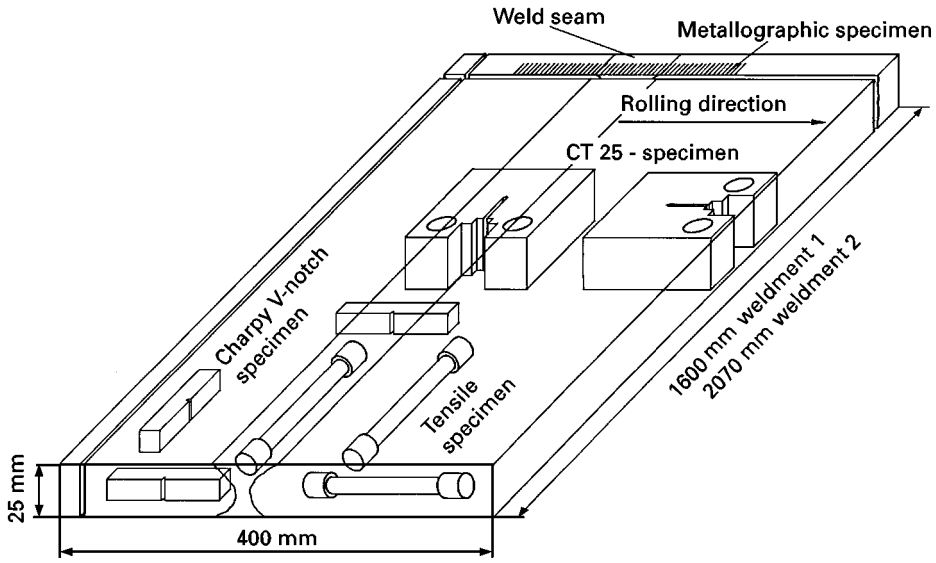

Figure 3 Type and orientation of specimens tested.

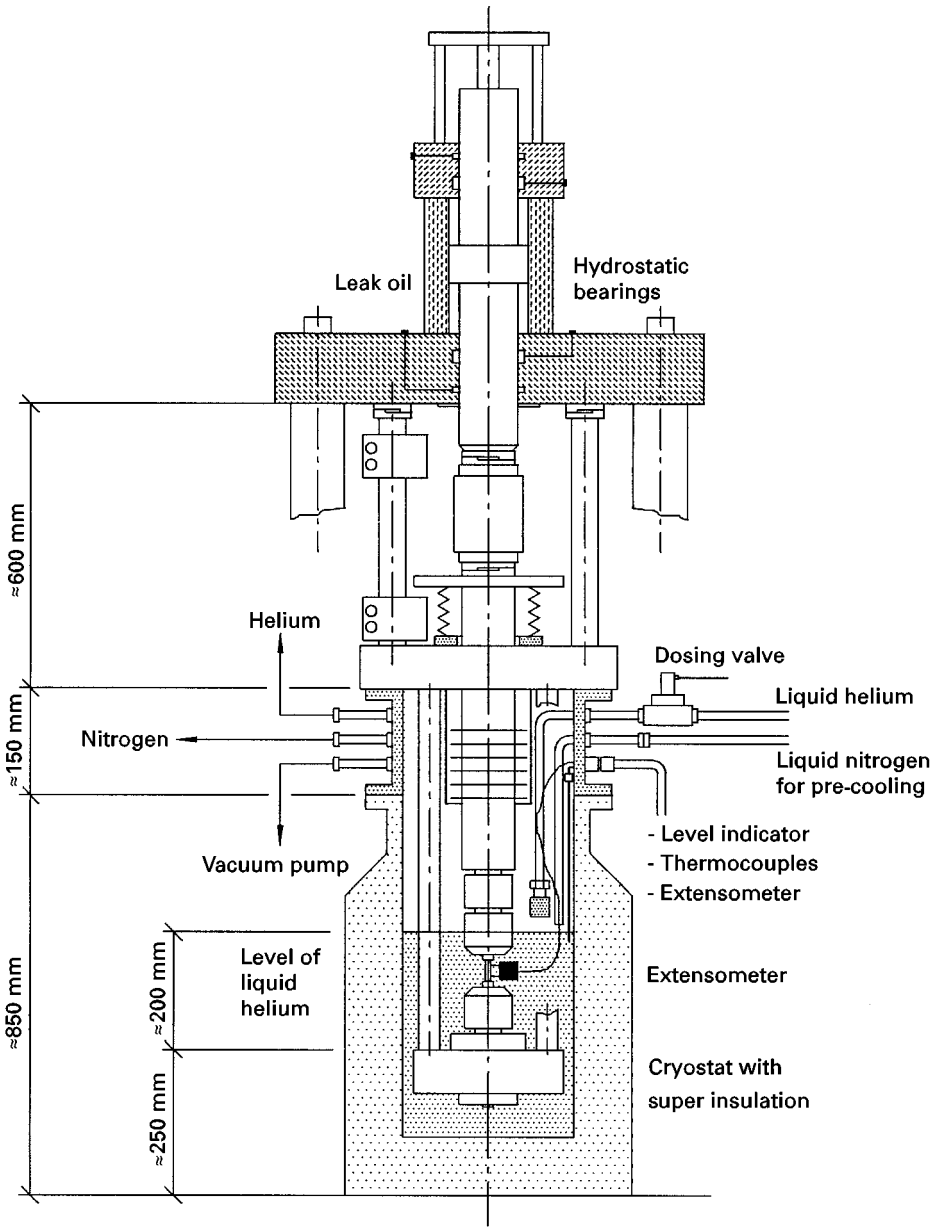

Figure 4 Low-temperature materials testing system.

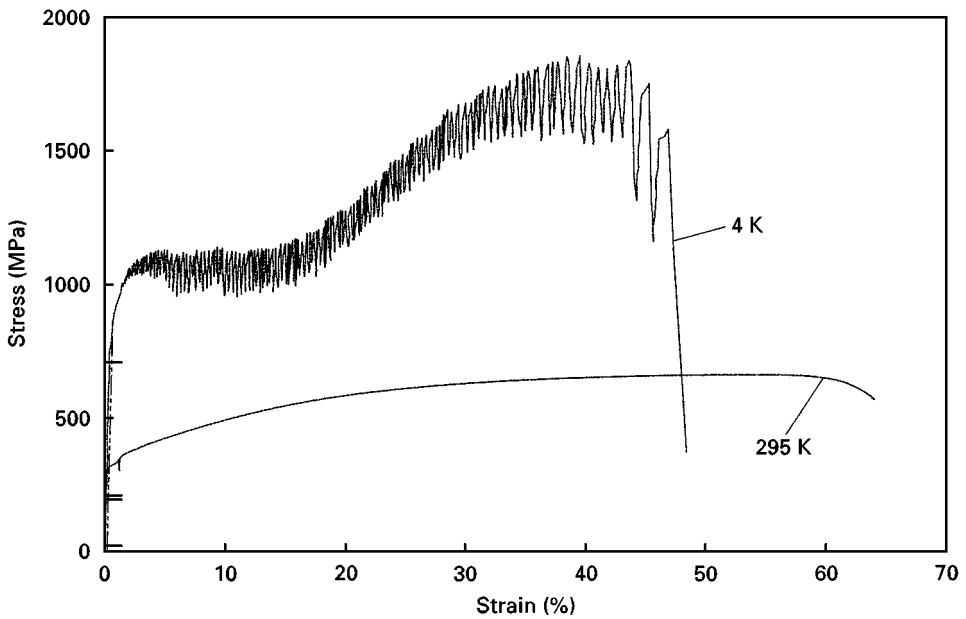

Figure 5 Stress–strain curves of steel X2 CrNiN 18 10 (similar to AISI 304 LN) at 295 and 4 K ($\dot{\varepsilon} = 5 \times 10^{-4}\,s^{-1}$).

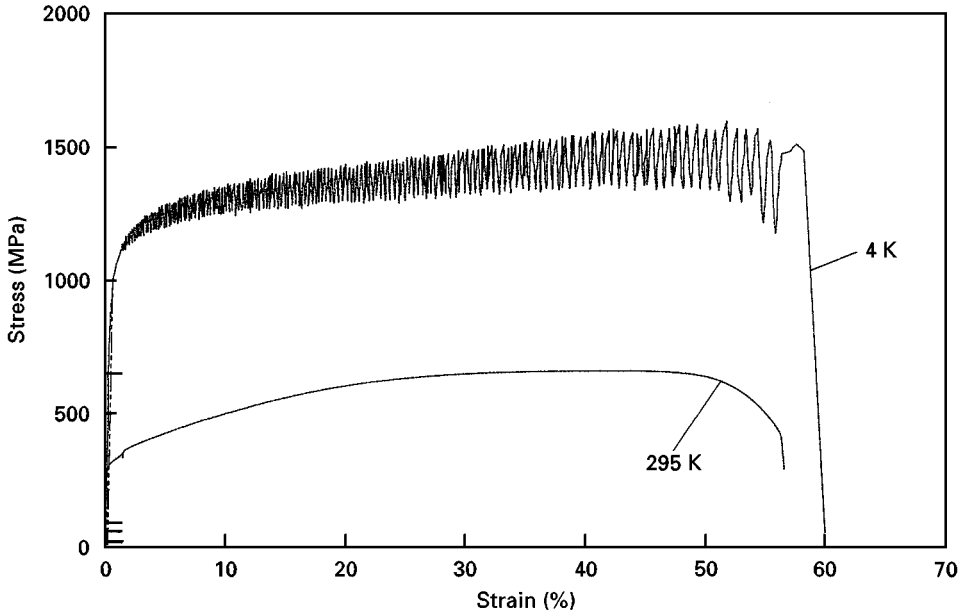

Figure 6 Stress–strain curves of steel X 4 CrNiMoN 18 14 (similar to AISI 316 LN) at 295 and 4 K ($\dot{\varepsilon} = 5 \times 10^{-4}\,s^{-1}$).

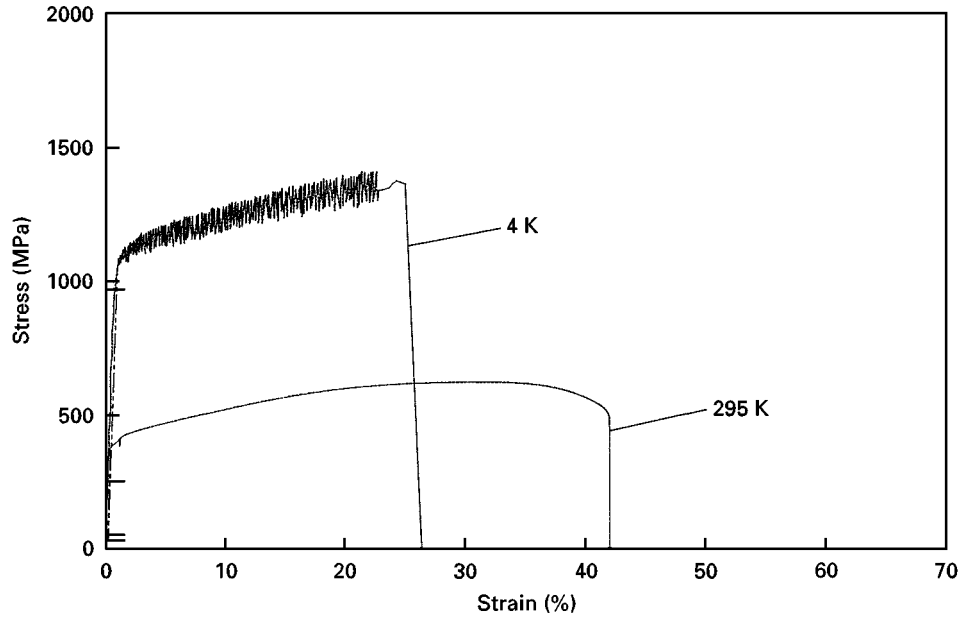

Figure 7 Stress–strain curves of weld metal X 2 CrNiMnMoN 20 16 at 295 and 4 K ($\dot{\varepsilon} = 5 \times 10^{-4}\,s^{-1}$).

fracture shows a maximum at 77 K and even at 4 K the value is higher than at room temperature, whereas the reduction in area decreases with decreasing temperature. With regard to specimen orientation, differences in the tensile properties of the base materials were only marginal, except for the reduction in area at 4 K for the steel X 2 CrNiN 18 10 which shows a significantly lower value in the case of the transverse specimen. The tensile properties of the weld metal of the two weld seams show only minor differences between the two weldments. The strength values are similar to the values of the steel X 4 CrNiMoN 18 14 but the elongation at fracture and reduction in area are much lower than for the base materials.

3.2. Impact testing

The results of the impact tests given in Fig. 11 show that, at all three temperatures, the base materials have a significantly higher absorbed energy than the weld metal. With decreasing temperature the absorbed energy decreases but, even at 4 K, values of 209 J and 115 J for the base materials and 60 J for the weld metal are achieved. It should be borne in mind that at 4 K the impact test is quasiadiabatic and that the actual temperature of the specimen can rise from 4 K at the start of the test to the predicted approximately 150 K for austenitic stainless steels at the end of the test [20]. According to [20], the meaning of Charpy impact tests at liquid-helium temperature is questionable and it is concluded there that it is not possible to estimate

TABLE III Results of the tensile tests at different temperatures

Material	Temperature (K)	Orientation[a]	Yield strength, $R_{p0.2}$ (N mm^{-2})	Tensile strength, R_m (N mm^{-2})	Elongation at fracture A(%)	Reduction in area, Z(%)
Base material	295	L	314	628	51	80
X 2 Cr NiN		T	307	625	51	75
18 10		L	715	1595	45	51
(similar to 304 LN)	77	T	711	1604	44	54
		L	865	1858	45	50
	4	T	828	1925	42	38
Base material	295	L	298	658	45	78
X 4 CrNiMoN		T	326	652	46	79
18 14	77	L	744	1319	59	68
(similar to 316 LN)		T	813	1312	60	67
	4	L	—	—	—	—
		T	992	1599	55	50
Weld metal	295	L	412	628	41	58
X 2 CrNiMnMoN	77	L	837	1243	39	33
20 16	4	L	1047	1419	21	25

[a] L, longitudinal specimens with respect to rolling direction of the plate or welding direction; T, transverse specimens with respect to rolling direction of the plate.

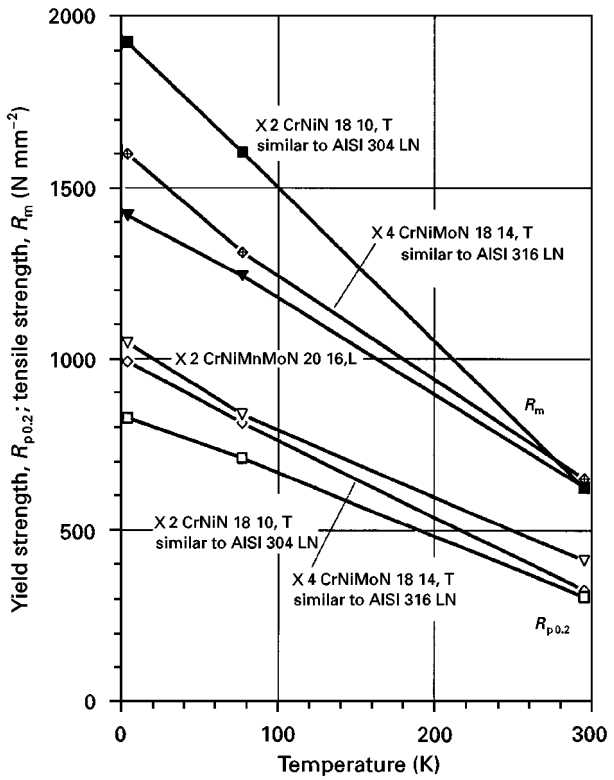

Figure 8 Yield and tensile strengths of the base materials and the weld metal at 295, 77 and 4 K. L, longitudinal; T, transverse.

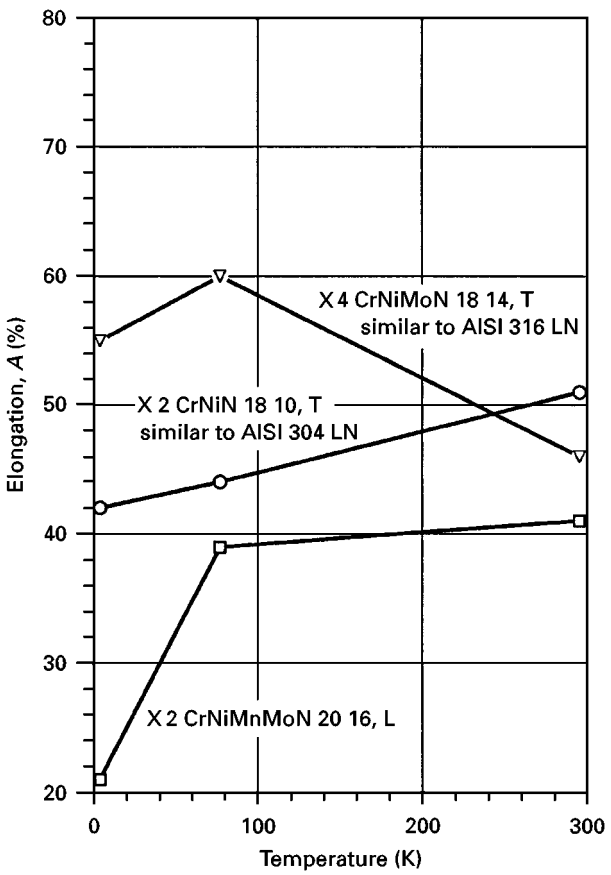

Figure 9 Elongation at fracture of the base materials and the weld metal at 295, 77and 4 K. L, longitudinal; T, transverse.

accurately the 4 K fracture toughness of ductile steels using Charpy impact tests.

3.3. Fracture mechanics

The J–R curves received for the three materials at room temperature, 77 K and 4 K were approximated by a polynomial in accordance with DVM 002 [14] and are shown in Figs 12–14. They reveal that with decreasing temperature the slope of the J–R curve is reduced, i.e., the lower the temperature, the lower is the J value for a given crack extension Δa. Only in the case of the steel X 4 CrNiMoN 18 14 does a small part

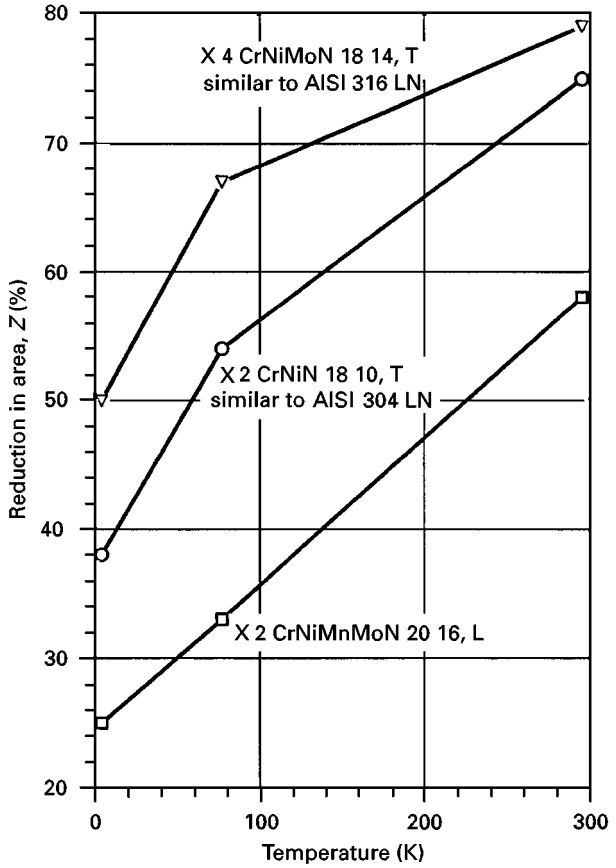

Figure 10 Reduction in area at fracture of the base materials and the weld metal at 295, 77 and 4 K. L, longitudinal; T, transverse.

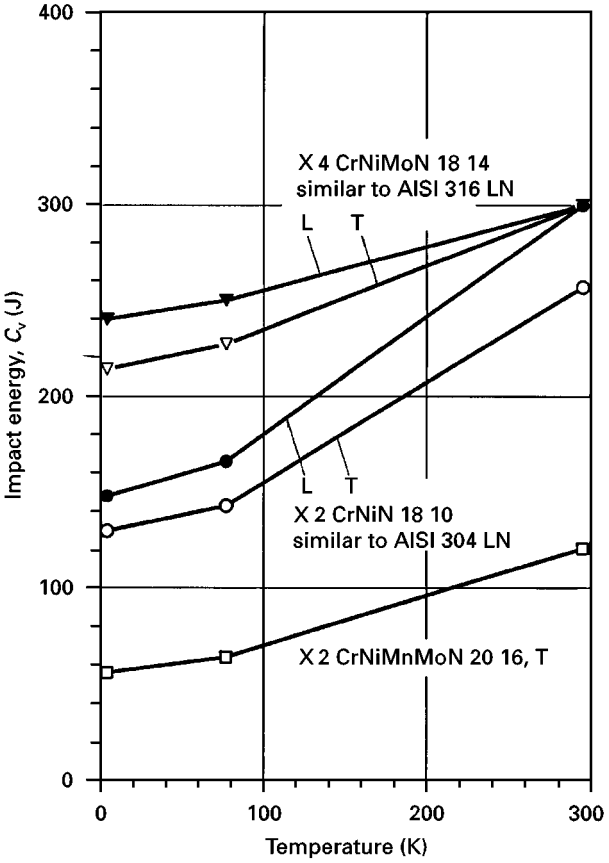

Figure 11 Impact energy of the base materials and the weld metal at 295, 77 and 4 K. L, longitudinal; T, transverse.

of the *J–R* curve for 77 K lie above the room-temperature curve. The *J–R* curves for 4 K are always situated below the *J–R* curves recorded for 77 K. This clearly indicates that it is necesary to test at 4 K if the fracture mechanics properties at this temperature are needed for a safety evaluation. Comparing the *J–R* curves for the three materials at 4 K, Fig. 15 shows that the steel X 4 CrNiMoN 18 14 has the best crack resistance behaviour and that the weld metal is slightly superior to the Steel X 2 CrNi 18 10.

The critical values, J_{Ic}, for the *J* integral evaluated according to ASTM E 813-81 [12], ASTM E 813-89

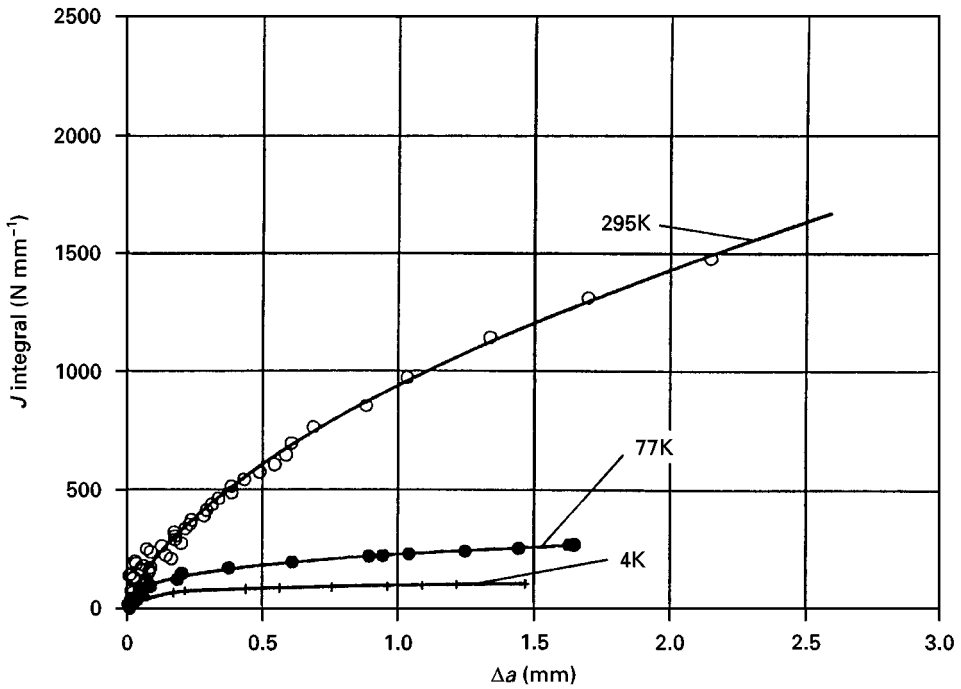

Figure 12 *J–R* curves of steel X 2 CrNiN 18 10 (similar to AISI 304 LN) at 295, 77 and 4 K.

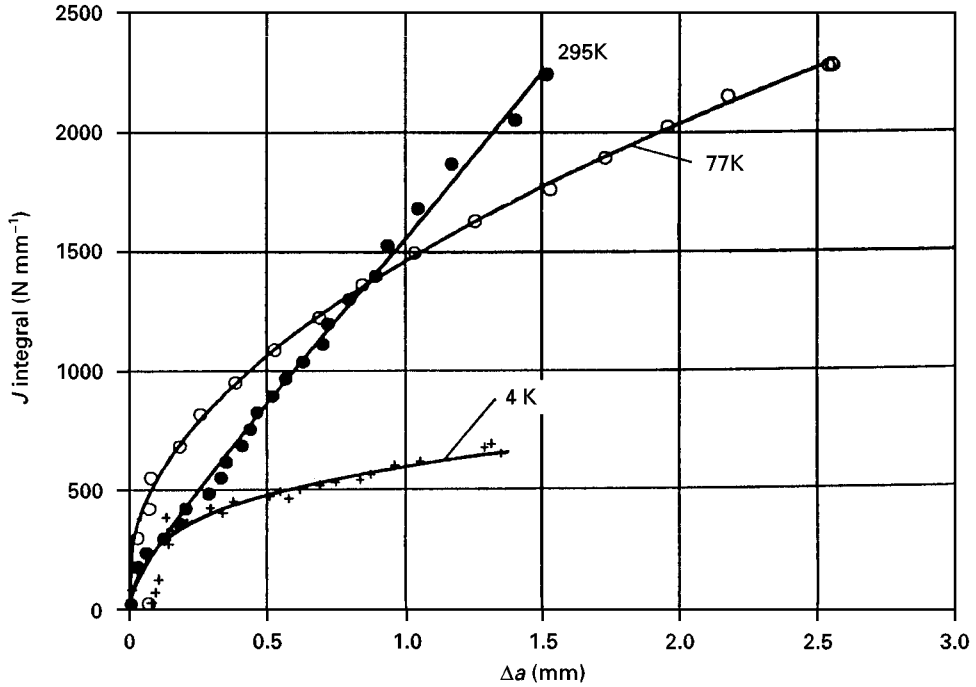

Figure 13 *J–R* curves of steel X 4 CrNiMoN 18 14 (similar to AISI 316 LN) at 295, 77 and 4 K.

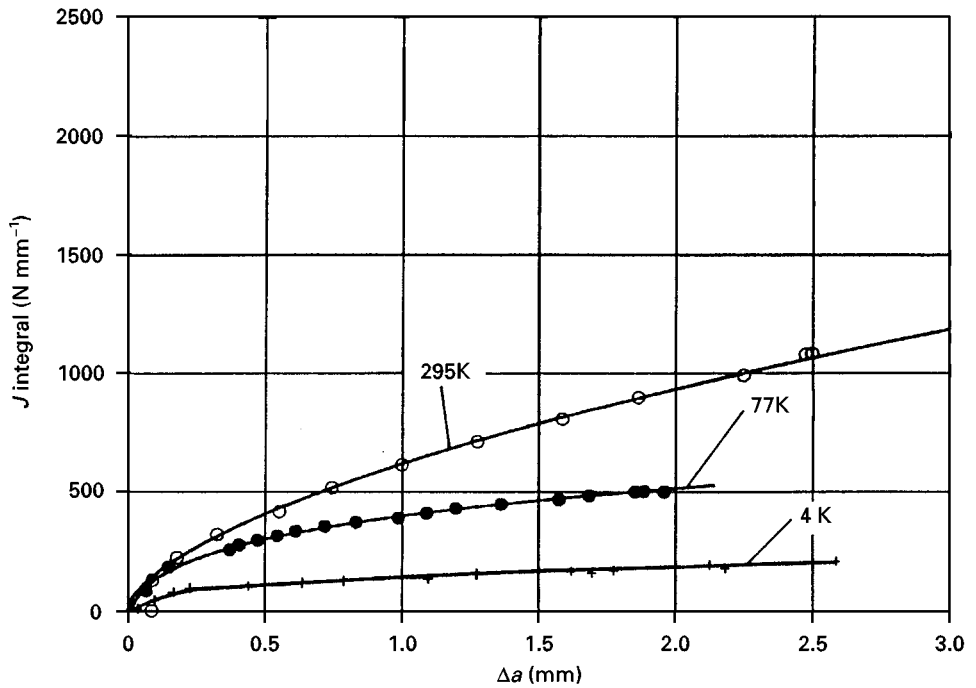

Figure 14 *J–R* curves of weld metal X 2 CrNiMnMoN 20 16 at 295, 77 and 4 K.

[13] and DVM 002 [14] listed in Table IV together with the measured values for the stretch zone also show the superior behaviour of the steel X 4 CrNiMoN 18 14. At room temperature it was not possible to apply ASTM E 813-81 [12] and ASTM E 813-89 [13] because several validation criteria such as thickness and initial ligament criterion and restrictions concerning J_{max} were not met. The J_{Ic} value generally decreased with decreasing temperature. The J_i values were significantly lower (by a factor of approximately 2) than the J_{Ic} values in the case of valid tests. In order to compare the J_{Ic} values with published $K_{Ic}(J)$ values at 4 K, the J_{Ic} values according to ASTM E 813-89 [13] listed in Table IV for this temperature were converted to $K_{Ic}(J)$ using the relation $K_{Ic}(J) = [EJ_{Ic}/(1 - \nu^2)]^{1/2}$, where $K_{Ic}(J)$ corresponds to fracture toughness near the onset of slow stable crack growth, E is the modulus of elasticity and ν Poisson's ratio. These values are compared with the well-known scatter bands for the dependence of $K_{Ic}(J)$ on the yield strength for base materials and weld metals [21] in Fig. 16. This comparison shows that the $K_{Ic}(J)$ value of the steel X 4 CrNiMoN 18 14 is located slightly above the scatter band for type 316

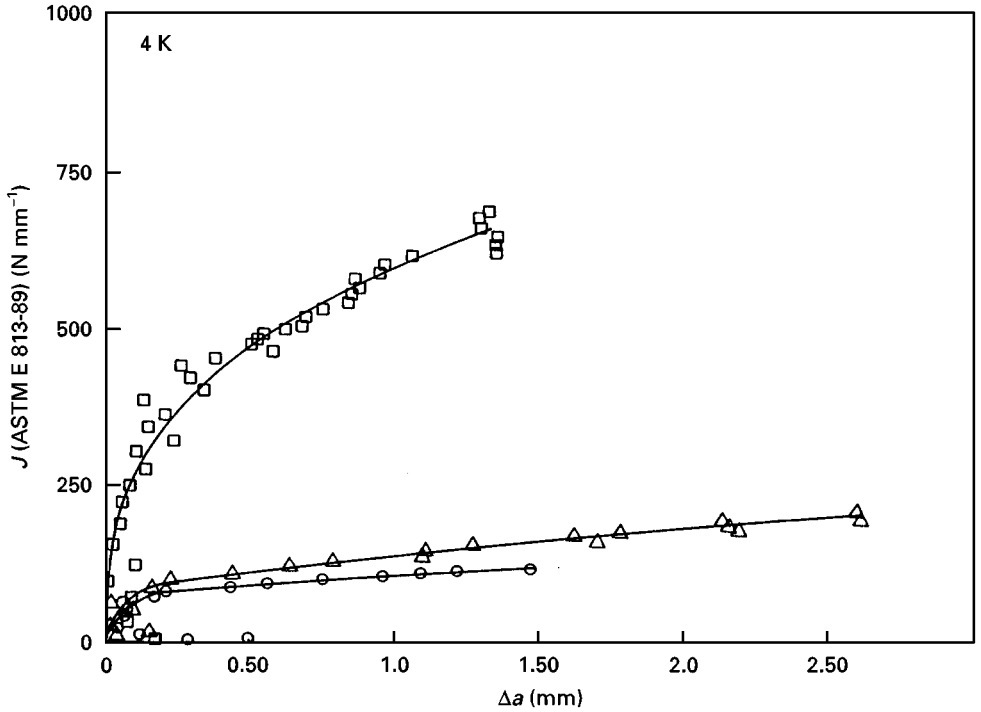

Figure 15 Comparison of the J–R curves of the base materials and the weld metal at 4 K. (○), X 2 CrNiN 18 10; (□), X 4 CrNiMoN 18 14, (△) X 2 CrNiMnMoN 20 16.

TABLE IV Results of J-integral tests on the base materials and the weld metal at 295, 77 and 4 K evaluated in accordance to different specifications

Material	Temperature (K)	ASTM 813-81, J_{Ic}(N mm^{-1})	ASTM 813-89, J_{Ic}(N mm^{-1})	DVM 002	
				J_i(N mm^{-1})	Δa_i[a](mm)
Base material	295	—[b]	1235[c]	327[c]	0.200
X 2 CrNiN 18 10	77	152	153	75	0.044
(similar to 304 LN)	4	71	72	30	0.011
Base material	295	—[b]	—[b]	399[c]	0.188
X 4 CrNiMoN 18 14	77	1285[c]	782[c]	706[c]	0.195
(similar to 316 LN)	4	368	392	247	0.115
Weld metal	295	416[c]	450[c]	150	0.098
X 2 CrNiMnMoN 20 16	77	241	254	92	0.061
	4	86	90	40	0.012

[a] Δa_i is the stretch zone width.
[b] —, some validation criteria not fulfilled.
[c] Thickness criterion not fulfilled.

base materials and that the X 2 CrNiMnMoN 20 16 weld metal is situated at the upper limit of the corresponding scatter band. The $K_{Ic}(J)$ value of the steel X 2 CrNiN 18 10 is well below the trend line for type 304 base material [5]. As the fracture toughness of austenitic strainless steel increases with increasing nickel content [22], this deviation will mainly result from the fact that this trend line is based on tests of compositions which have a higher nickel content (9.91–10.10 wt%) than the composition tested in this investigation with 9.06 wt% nickel. Decreasing the nickel content can reduce the austenite phase stability of 304 N steel, leading to easier transformation to martensite. This is in consequence can adversly affect the ductility.

3.4. Fractography

The fracture surface of the tensile specimens of the steel X 2 CrNiN 18 10 tested at room temperature and at 77 K is characterized by a ductile cup-and-cone fracture, the dimples in the centre being larger and deeper at room temperature. The tensile specimens tested at 4 K had a rather plain fracture surface with shallow small dimples (Fig. 17). The tensile specimens of the steel X 4 CrNiMoN 18 14 had a higher ductility at all testing temperatures than did the steel X 2 CrNiN 18 10. Even at 4 K, large dimples with non-metallic inclusions were observed (Fig. 18). The elliptical shape of the macroscopic fracture surface of the all-weld metal specimens was indicative of a certain anisotropy. At all testing temperatures, medium-size

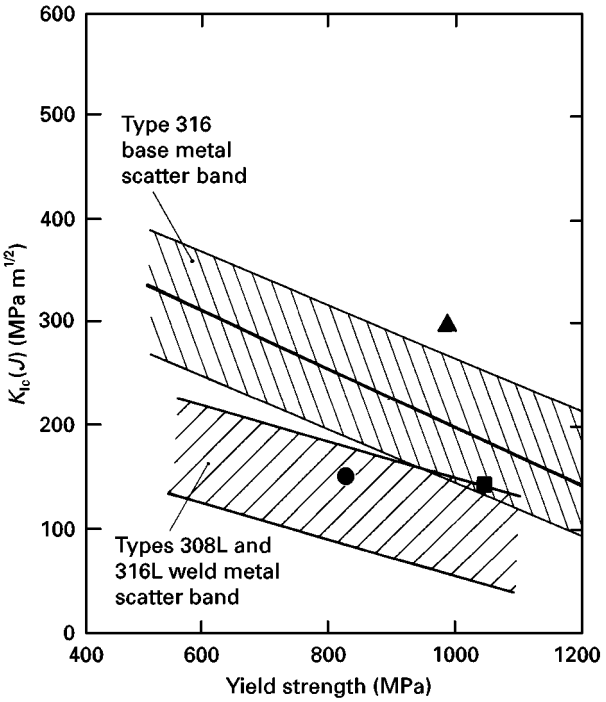

Figure 16 Comparison of the results of this investigation at 4 K with literature data for variable N content (type 304 base metal trend line according to [5]; scatter bands for type 316 base metal and types 308L and 316L weld metal according to [21]). (●), X 2 CrNiN 18 10 (similar to AISI 304 LN); (▲), X 4 CrNiMoN 18 14 (similar to AISI 316 LN); (■), X 2 CrNiMnMoN 20 16; (——), type 304 base metal trend line.

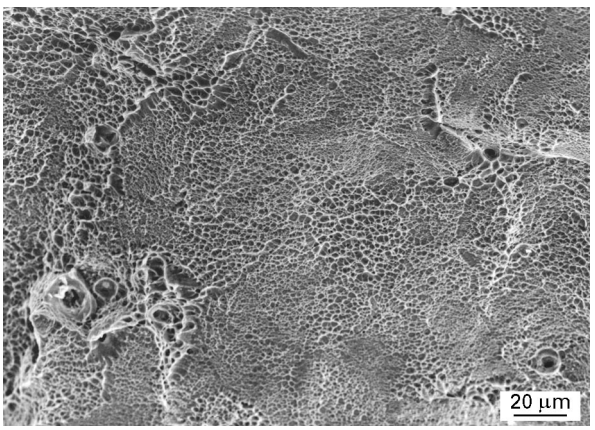

Figure 17 SEM fractograph of tensile specimen of X 2 CrNiN 18 10 tested at 4 K.

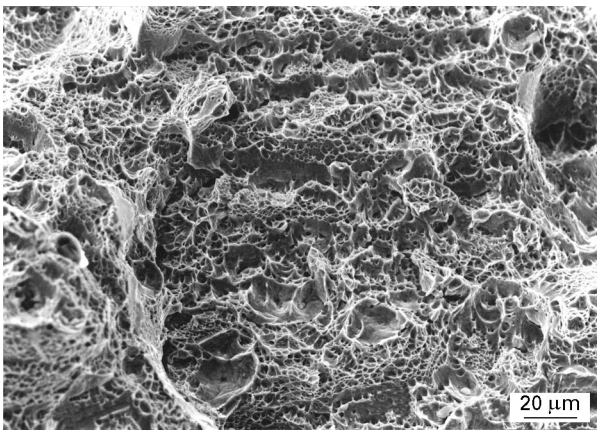

Figure 18 SEM fractograph of tensile specimen of X 4 CrNiMoN 18 14 tested at 4 K.

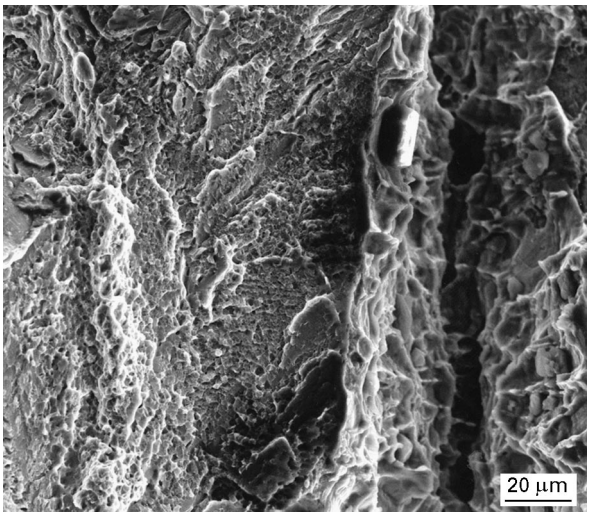

Figure 19 SEM fractograph of stable crack growth region of the compact tension specimen of steel X 2 CrNiN 18 10 tested at 4 K.

dimples were visible which became flatter with decreasing testing temperature.

The fracture surfaces of the CVN impact toughness specimens show similar tendencies with regards to the size and depth of the dimples as for the tensile specimens. The CVN specimens of the weld metal had a more inhomogeneous macroscopic fracture surface resulting from the structure of the welding. On a macroscopic scale, mainly small- to medium-size dimples, frequently containing non-metallic inclusions, were found.

The marked reduction in J_{Ic} and J_i values with decreasing temperature was clearly reflected in the appearance of the fracture surface of the compact tension specimens. The steel X 2 CrNiN 18 10 tested at room temperature shows a broad stretch zone and a stable crack advance with large dimples. At 77 K the width of the stretch zone is reduced and the stable crack growth is plainer with a certain orientation parallel to the main deformation direction of the material and smaller dimples. The stretch zone of the 4 K specimen can only be identified on certain parts along the width of the specimen. Within the stable crack growth region, which is flatter than at 77 K and consists of small dimples, regions with low deformation are found (Fig. 19). In the case of the steel X 4 CrNiMoN 18 14 the fracture surfaces of the specimens tested at room temperature and 77 K are rather similar. A broad stretch zone is found and the stable crack growth region appears macroscopically rough with large deep dimples visible at a higher magnification. At the testing temperature of 4 K the width of the stretch zone is significantly reduced as also are the number and depth of large dimples (Fig. 20).

The fracture surfaces of the specimens from the weld metal X 2 CrNiMnMoN 20 16 are influenced by the inhomogeneity of the structure of the weld metal. The specimen tested at room temperature has a stretch zone containing numerous small slip lines. The stable crack growth region consists of a rough structure of medium-sized dimples in which frequently non-metallic

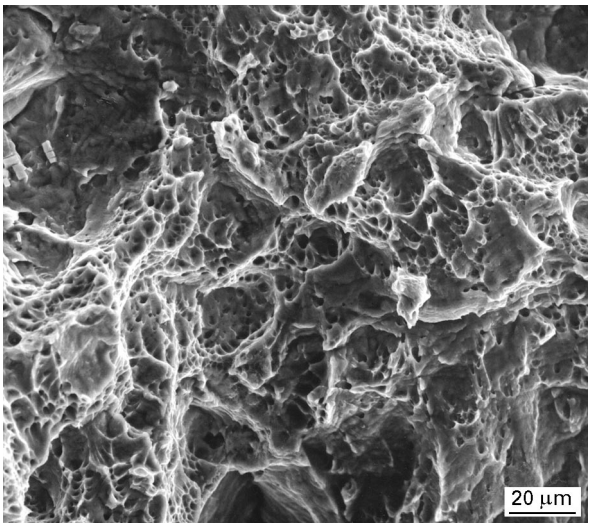

Figure 20 SEM fractograph of the stable crack growth region of the compact tension specimen of steel X 4 CrNiMoN 18 14 tested at 4 K.

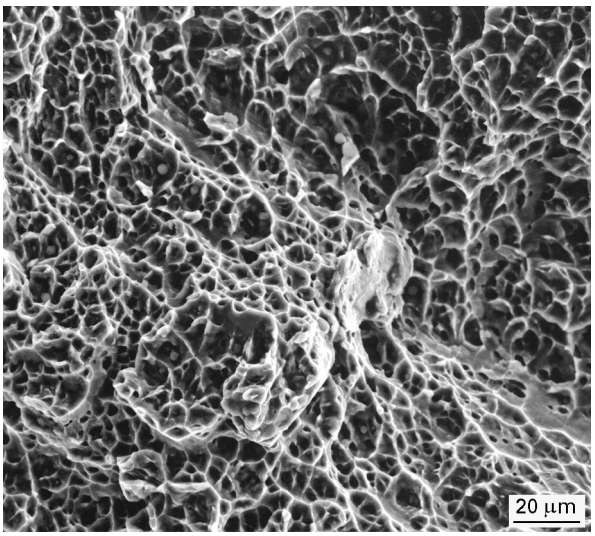

Figure 21 SEM fractograph of the stable crack growth region of the compact tension specimen of the weld metal X 2 CrNiMoN 20 16 tested at 4 K.

inclusions are observed. The stretch zone at 77 K is a narrow region of varying width without slip lines. The mean size and depth of the dimples are reduced. At a testing temperature of 4 K the stretch zone is very narrow with local interruptions. The stable crack growth region appears macroscopically as a dim stripe consisting microscopically of medium-size dimples often containing non-metallic inclusions (Fig. 21).

4. Summary and conclusions

The results of this investigation can be summarized as follows.

1. With decreasing temperature, the yield and tensile strength of both base materials X 2 CrNiN 18 10 and X 4 CrNiMoN 18 14 as well as the weld metal X 2 CrNiMnMoN 20 16 increased significantly. The reduction in area was lessened to a similar degree for all materials, whereas the elongation at fracture was reduced significantly only in the case of the weld metal.

2. At all three test temperatures (295, 77 and 4 K) the Charpy impact energy of the weld metal was significantly lower than the impact energy of the base materials.

3. For all three materials (two base materials and one weld metal) and at all the temperatures, where the validation criterias are fulfilled the J_{Ic} values according to ASTM E 813-81 [12] and ASTM E 813-89 [13] are approximately twice the J_i values for physical crack initiation according to DVM 002 [14].

4. At 4 K the J_i values of the base material X 2 CrNiN 18 10 and the weld metal are of the same order of magnitude and are reduced by a factor of approximately two compared with the values at 77 K. In contrast the base material X 4 CrNiMoN 18 14 has a markedly higher J_i value at both 77 K and 4 K.

5. A good combination of strength and toughness can be achieved using the SA weld process.

In conclusion it was clear that for a reliable database for analysing and evaluating the behaviour of components at liquid-helium or liquid-hydrogen temperature using fracture mechanics it is not sufficient to determine these data at 77 K only. In the case of liquid hydrogen, the possibility of degradation due to the influence of the medium has to be considered and the relevance of this possible influence could be proven by materials tests in liquid hydrogen.

Acknowledgements

The authors acknowledge the financial support of the German Ministry of Research and Technology, the supply of the base materials and the weldments by Thyssen Nordseewerke, Emden, Germany, the performance of the impact test at 4 K by Linde, Höllriegelskreuth, Germany, as well as the project management by Deutsche Gesellschaft für Chemisches Apparratewesen, Chemische Technik und Biotechnologie e.V., Frankfurt, Germany.

References

1. F. J. EDESKUTY and K. D. WILLIAMS, in "Hydrogen: its technology and implications", Vol. II, edited by K. E. Cox and K. D. Williamson Jr (CRC Press, Cleveland, OH, 1977) Chap. 3, p. 51.
2. P. DEIMEL, M. HOFFMANN and H. FISCHER, in Proceedings of the Deutsche Kälte-Klima-Tagung 1995, Ulm, 22–24 November 1995, Deutscher Kälte- und Klimatechnischer Verein Tagungsbericht 22, Vol. I (1995) p. 53.
3. H. I. McHENRY, in "Materials at low temperatures", edited by R. P. Reed and A. F. Clark (American Society for Metals, Metals Park, OH, 1983) p. 371.
4. G. H. EICHELMANN and F. C. HULL, *Trans. Amer. Soc. Metals* **45** (1953) 77.
5. R. L. TOBLER, D. T. READ and R. P. REED, ASTM Special Technical Publication 743, edited by R. Roberts (American Society for Testing Materials, Philadelphia. PA (1981) p. 250.
6. R. P. REED, N. J. SIMON, P. T. PURTSCHER and R. L. TOBLER, in "Materials studies for magnetic fusion energy applications at low temperatures IX", NBSIR-86 3050, edited by R. P. Reed (National Bureau of Standards, Boulder, CO, 1986) p. 15.
7. R. L. TOBLER, T. A. SIEWERT and H. I. McHENRY, *Cryogenics* **26** (1986) 392.
8. C. N. McCOWAN, T. A. SIEWERT and R. L. TOBLER, *Trans. ASME* **108** (1986) 340.

9. D. T. READ, H. I. McHENRY, P. A. STEINMEYER and R. D. THOMAS Jr, *Welding J.* **59** (1980) 104s.
10. T. A. WHIPPLE and D. J. KOTEKI, in "Materials studies for magnetic fusion energy applications at low temperatures IV", NBSIR-81 1645, edited by R. P. Reed and N. J. Simon (National Bureau of Standards, Boulder, CO, 1981) p. 303.
11. T. A. WHIPPLE, H. I. McHENRY and D. T. READ, *Welding J.* **60** (1981) 77s.
12. ASTM Standard E 813-81 (American Society for Testing and Materials, Philadelphia, PA, 1981).
13. ASTM standard E 813-89 (American Society for Testing and Materials, Philadelphia, PA, 1989).
14. DVM 002 (German Association for Testing Materials, Berlin, 1987).
15. P. DEIMEL, H. FISCHER and M. HOFFMANN, in Proceedings of the 11th World Hydrogen Energy Conference, Stuttgart, 23–28 June 1996, Vol. 3, edited by T. N. Veziroglu, C.-J. Winter, J. P. Baselt and G. Kreysa (International Association for Hydrogen Energy, Coral Gables, FL, 1996) p. 2303.
16. DIN EN 1002-1 (Deutsches Institut für Normung, Berlin, 1991).
17. ASTM Standard E. 1450-92 (American Society for Testing and Materials, Philadelphia, PA, 1992).
18. DIN EN 10045 (Deutsche Institut für Nomung, Berlin, 1991).
19. R. P. REED and R. L. TOBLER, *Adv. Cryogenic Engng Mater.* **28** (1982) 49.
20. R. L. TOBLER, R. P. REED, I. S. HWANG, M. M. MORRA, R. G. BALLINGER, H. NAKAJIMA and S. SHIMAMOTO, *J. Testing Eval.* **19** (1991) 34.
21. T. A. SIEWERT and C. N. McCOWAN, *Adv. Cryogenic Engng Mater.* **38** (1992) 109.
22. R. P. REED, P. T. PURTSCHER and K. A. YUSHENKO, *ibid* **32** (1986) 43.

Received 28 June 1996
and accepted 20 August 1997